

EgoCogNav: Cognition-aware Human Egocentric Navigation

Zhiwen Qiu¹ Ziang Liu¹ Wenqian Niu¹ Tapomayukh Bhattacharjee¹ Saleh Kalantari¹
¹Cornell University

Abstract

Modeling the cognitive and experiential factors of human navigation is central to deepening our understanding of human–environment interaction and to enabling safe social navigation and effective assistive wayfinding. Most existing methods focus on forecasting motions in fully observed scenes and often neglect human factors that capture how people feel and respond to space. To address this gap, We propose EgoCogNav, a multimodal egocentric navigation framework that predicts perceived path uncertainty as a latent state and jointly forecasts trajectories and head motion by fusing scene features with sensory cues. To facilitate research in the field, we introduce the Cognition-Aware Egocentric Navigation (CEN) dataset consisting of 6 hours of real-world egocentric recordings capturing diverse navigation behaviors in real-world scenarios. Experiments show that EgoCogNav learns the perceived uncertainty that highly correlates with human-like behaviors such as scanning, hesitation, and backtracking while generalizing to unseen environments.

1. Introduction

Understanding human navigation processes is fundamental to safe, reliable human–environment and human–machine interactions [15, 48]. Humans perceive their environments from egocentric perspectives to inform decision-making for subsequent motions. Learning such cues is crucial for applications including autonomous driving [22, 56], social robot navigation [38, 50, 57], and assistive wayfinding systems [12, 44, 61].

Modeling human navigation requires not only accurate scene representation and motion forecasting, but also human factors that capture how people experience and emotionally respond to built environments, which are closely related to productivity, satisfaction, and well-being [11, 24, 34, 47]. Incorporating these cognitive states into behavioral models can deepen our understanding of interacting with environments and substantially enhance their utility for salient environmental design and personalized navigation assistance in complex settings [10, 24]. Perceived un-

certainty, defined as a state in which an individual is trying to decide between alternative courses of action, is a driver of wayfinding behaviors tied to discomfort and negative emotions [10, 20, 45]. Predicted uncertainty levels can inform probabilistic wayfinding behaviors as well as a valuable metric for understanding users’ experience of a space. However, most prior work in human trajectory prediction does not account for cognitive and psychological processes and rely instead on motion history and context for path forecasting [17, 23, 36], use rule- or agent-based methods [9, 37, 65], or develop socially compliant policies for navigation [19, 26, 40, 53]. Although some incorporate cognitive factors such as emotions, panic, and stress, these frameworks typically assume fully observed third-person or bird’s-eye-view (BEV) scenes and often planar worlds [6, 12, 44, 61]. Furthermore, there is limited multimodal egocentric navigation datasets, especially those with cognitive annotations, to study these effects at scale.

To address the challenges, we propose EgoCogNav, a multimodal egocentric navigation framework that jointly predicts perceived uncertainty, body-centered trajectories and head motion. The framework fuses first-person scene evidence from a pre-trained DINOv2 vision backbone [7, 42] with recent motion where cognition and behaviors are learned in a single perception–decision–action loop. For stability and generalization, we introduce auxiliary predictors of environment types (e.g., occlusion, crowding) and behaviors (e.g., hesitation, backtrack) that are tightly linked to contexts and actions with uncertainty. The design is modular and extensible for additional modality input with shared time-series forecasting module. Finally, we introduce the Cognition-Aware Egocentric Navigation (CEN) dataset that features rich multimodal streams from 17 participants across diverse indoor and outdoor scenes for human navigation research. Our contribution can be summarized as follows:

- We formalize cognition-aware egocentric forecasting task to jointly predict trajectory, head motion, and moment-to-moment perceived path uncertainty.
- We propose EgoCogNav, which fuses multiple sensory inputs with human-grounded uncertainty to produce behaviorally realistic behavior forecasts useful for assistive

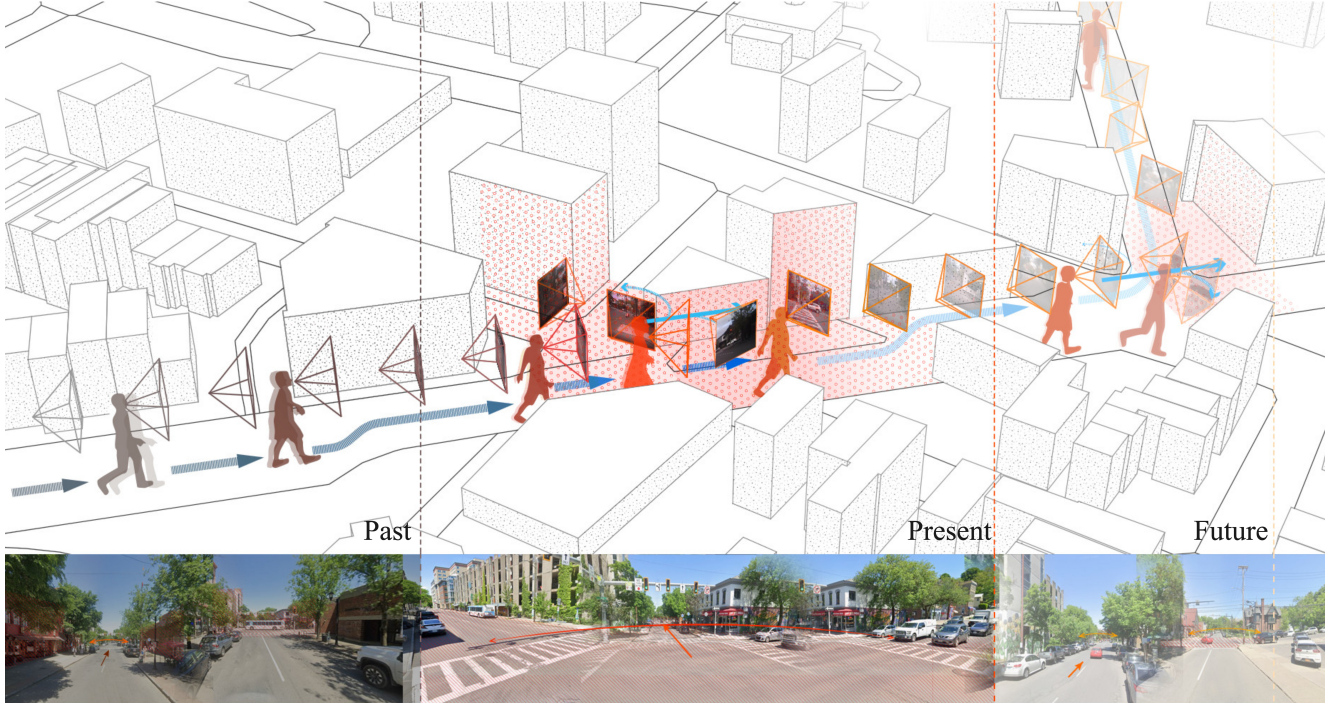


Figure 1. Given a past window of motion, head rotations, gaze, and navigational goal, our model jointly predicts a future body-frame trajectory, head poses, and the current state of perceived uncertainty. This setting reflects real-world navigation challenges in environments where the model must anticipate internal cognitive state and making decisions for subsequent head motion and movement.

navigation and environmental design.

- We introduce a dataset consisting of 6 hours of real-world human navigation sessions that covers 42 diverse sites and environmental conditions.

2. Related Work

Human trajectory prediction. The prospect of predicting pedestrian trajectories from third-person or BEV has been extensively studied. Prior methods include deterministic predictors that estimate one most likely path using scene information and social cues [2, 25, 49], and stochastic models that generate multimodal futures or full distributions from probabilistic frameworks such as diffusion models [4, 17, 36] and normalizing flows [35, 52]. However, third-person views often neglect first-person natural perceptual and cognitive signals, which can limit the development of high-fidelity modeling of human motion in cluttered environments [39]. Despite substantial progress in egocentric human motion estimation [1, 27, 55, 62], trajectory and motion forecasting that incorporate human cognitive states remain underexplored. Wang and colleagues [59] use a diffusion framework to generate multiple plausible future trajectories from RGB-D video with a learned visual-memory of the surroundings. Pan and colleagues [43] predict 6-DoF head poses to learn collision-aware, information-

seeking behaviors by projecting 3D-feature volumes into BEV. However, these approaches largely assume homogeneous behaviors and overlook individual differences and internal cognitive states that are salient in real-world navigation. Integrating experiential factors can reveal why and when people hesitate or backtrack to improve behavioral fidelity and enable assistance and design interventions that anticipate difficulties rather than merely reacting to observed motion.

Perceived uncertainty in human wayfinding models. Perceived path uncertainty is a key cognitive variable that closely linked to wayfinding performance which emerges from limited knowledge about forthcoming events [10, 45]. The Entropy Model of Uncertainty (EMU) [20] posits that uncertainty is affected by the range of perceived choices and peak when perceived probability for each choice is equal. Prior strategies to integrate human cognition typically include translating empirical observations like “go-to” affordances into rule-based deterministic models [47], or defining utility parameters such as path choice and individual preference for agents to optimize during navigation [21, 60, 64]. For instance, Huang and colleagues [21] present a two-layer floor-field cellular automaton with three intertwined sub-modules (exit choice, locomotion, and exit-choice switching) to model risk- and uncertainty-aware decisions to capture pedestrian dynamics. Yang and col-

leagues [61] introduce a probabilistic data-driven wayfinding agent that integrates isovist-derived spatial metrics, signage visibility/recency, route-choice counts, and individual factors to predict continuous perceived path uncertainty for simulating human trajectories in indoor settings. In contrast to prior BEV- or rule-based formulations, we employ a data-driven and learning-based method that predicts perceived path uncertainty from multimodal first-person cues.

Egocentric dataset for human navigation. Many egocentric datasets [8, 16, 29, 32] provide real-world monocular RGB videos of diverse daily activities such as household, workplace, and outdoor scenes. To enrich human sensory inputs, subsequent efforts were made to incorporate wearable and instrumented platforms like motion-capture suits and Project Aria glasses [13] to deliver calibrated multimodal signals, including head poses [43, 58], gaze [28, 32], hand and object tracking [5, 54], full-body motion [33], and detailed scene and action annotations [30]. However, these datasets are not explicitly curated for human navigation. Few works utilized synthetic pipelines to simulate virtual human navigation and collisions in 3D environments from multi-view body-mounted cameras, but resulting motions are often simplified or unnatural due to constraints in existing motion generation methods. Closer to our setting, Wang and colleagues [59] and Pan and colleagues [43] develop egocentric human-navigation datasets, yet the coverage is comparatively limited and the focus is primarily trajectory or head-pose forecasting without leveraging varied sensory inputs or human cognitive factors. Moreover, neither dataset is publicly released to date. Therefore, we introduce a new dataset that unifies sensory signals, cognitive indicators, and accurate localization across diverse indoor and outdoor scenes.

3. Method

3.1. Problem formulation

As illustrated in Fig. 1, our problem formulation can be expressed as given a past egocentric video $\mathbf{X}_{1:T_1} \in \mathbb{R}^{T_1 \times H \times W \times 3}$, past body-frame motion $\mathbf{S}_{1:T_1} = [\Delta x, \Delta y, \Delta \psi] \in \mathbb{R}^{T_1 \times 3}$, 6D continuous head rotations [63] $\mathbf{H}_{1:T_1} \in \mathbb{R}^{T_1 \times 6}$, normalized gaze points $\mathbf{G}_{1:T_1} \in \mathbb{R}^{T_1 \times 2}$, and body-frame navigation goals $\mathbf{Q}_{1:T_1} = [d, \sin \beta, \cos \beta] \in \mathbb{R}^{T_1 \times 3}$, our goal is to jointly predict the future trajectory $\hat{\mathbf{S}}_{T_1+1:T_1+T_2} \in \mathbb{R}^{T_2 \times 3}$, head-pose sequence $\hat{\mathbf{H}}_{T_1+1:T_1+T_2} \in \mathbb{R}^{T_2 \times 6}$, and the current perceived uncertainty $\hat{U}_{T_1} \in [0, 1]$. At 10Hz, we use a past window $T_1 = 30$ steps (3s) and $T_1 = 10$ steps (1s).

3.2. EgoCogNav Architecture

Our framework is organized into three modules: (1) a perception module that extracts spatio-temporal features from recent video using a pre-trained vision transformer, (2) an

action module that encodes past body-frame motion, head rotation and gaze together with goal conditioning, and (3) a cognitive module that outputs cognitive value in the current internal state. The perception and action streams are fused into a shared representation, where we then attach parallel temporal decoders for body-frame trajectory and head-motion forecasting, together with a cognition head that predicts uncertainty.

Perception module. The shared encoder works as the perceptual aspect that processes the past RGB frames. Each frame is resized to 224×224 and passed through a pre-trained vision transformer DINOv2 [7, 42] to produce a temporal stack of 2D feature maps $\mathbf{F}^{2D} \in \mathbb{R}^{T \times 16 \times 16 \times 384}$. These features are fed directly into the subsequent fusion and temporal forecasting modules.

Action module. We encode four synchronized cues over the past T_1 steps: body-frame trajectory deltas $\mathbf{S}_{1:T_1} = [\Delta x, \Delta y, \Delta z]$, head rotations $\mathbf{H}_{1:T_1}$, gaze points $\mathbf{G}_{1:K} = (u, v)$ in normalized image coordinates, and navigation goal $\mathbf{Q}_{1:T_1} = [d, \sin \beta, \cos \beta]$ expressed in the current head frame. All streams are timestamp-aligned given positional encoding, and embed to the same width before fusion.

Cognition module. Conceptually aligned with the EMU theory of competing scene interpretations and action choices [20], we model the agent’s current internal state as a single-step prediction of perceived uncertainty $\hat{U}_t \in [0, 1]$ as a state signal that summarizes moment-to-moment choice difficulty preceding behaviors. The cognition head operates on the fused representation \mathbf{F} by temporal mean-pooling followed by a lightweight MLP.

Motion and cognition prediction. We fuse modalities by first applying self-attention over the video stream to form a temporal context and then cross-attending to motion, head, and gaze inputs to produce a fused sequence \mathbf{F} . To inject the intent of tasks, we apply adaptive goal conditioning that mixes the fused features with a goal embedding $\mathbf{h}_t^{\text{goal}}$ through a learned per-timestep operator that bias towards goal-consistent evidence when \hat{U}_t is high (e.g., greater choice ambiguity), thereby reducing representational uncertainty:

$$\tilde{\mathbf{h}}_t = (1 - \hat{U}_t) \mathbf{h}_t^{\text{fuse}} + \hat{U}_t \mathbf{h}_t^{\text{goal}} \quad (1)$$

On top of these features, we attach two parallel temporal decoders with learnable future queries. Trajectory head uses a time-series decoder to predict a 3 degrees-of-freedom (DOF) body-frame sequence $\hat{\mathbf{S}}_{T_1+1:T_1+T_2}$, and the head-motion head mirrors this design to predict future head sequence $\hat{\mathbf{H}}_{T_1+1:T_1+T_2}$. The uncertainty head mean-pools \mathbf{F} to produce the single-step prediction \hat{U}_t at time t . During training, we also add lightweight auxiliary classifiers on intermediate features to predict environment type and behavioral events where they regularize the shared backbone.

Loss function. For trajectory prediction, we prioritize near-

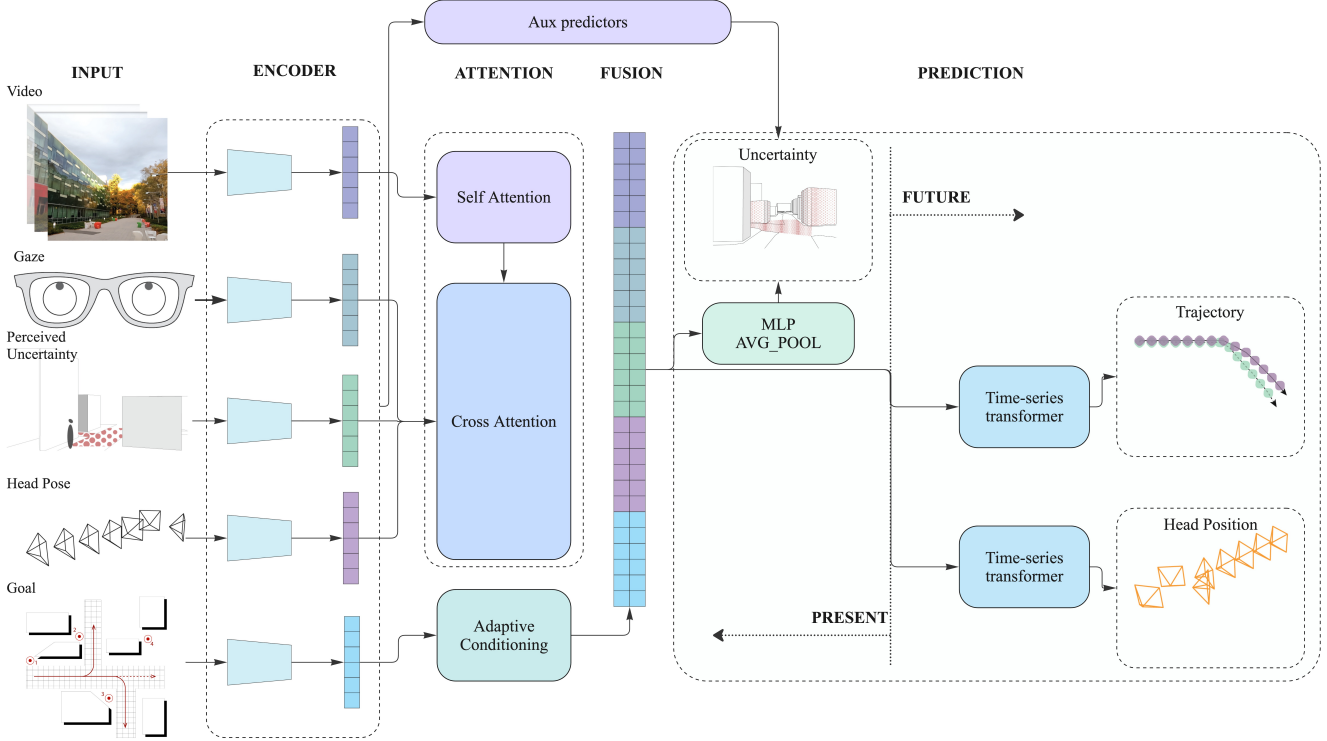


Figure 2. **EgoCogNav architecture.** Given a past egocentric video and sensory inputs, we fuse them into a shared representation with adaptive goal conditioning to jointly predict the current state of perceived uncertainty, future trajectory and head motion.

future steps [3] given a predicted sequence \mathbf{S}_{pred} and ground truth

$$\begin{aligned} \mathcal{L}_{\text{traj}} = & \sum_{i=1}^H \gamma^i \|(\mathbf{S}_{\text{pred}})_i - (\mathbf{S}_{\text{gt}})_i\|_1 \\ & + \lambda_{\text{var}} \left\| \text{std}_i(\mathbf{S}_{\text{pred}}) - \text{std}_i(\mathbf{S}_{\text{gt}}) \right\|_2^2 \end{aligned} \quad (2)$$

Where $\gamma \in [0.95, 0.99]$ and we use 0.98 in our experiments such that for $T_2=10$, the last step is weighted $0.98^{10} \approx 0.82$. The $\text{std}_i(\cdot)$ computes the per-dimension temporal standard deviation over $i=1:T_2$. Following previous work [43], head rotations use L1 loss where R_{t+i} is the rotation matrix and I is the identity matrix.

$$\mathcal{L}_{\text{head}} = \frac{1}{H} \sum_{i=1}^H \|\widehat{R}_{t+i} R_{t+i} - I\|_1 \quad (3)$$

We regress the human self-report perceived uncertainty at time t :

$$\mathcal{L}_U = \|\hat{U}_t - U_t^{\text{human}}\|_2^2. \quad (4)$$

The combined training loss is a linear combination of the three task losses and a small auxiliary term:

$$\mathcal{L}_{\text{total}} = \lambda_{\text{traj}} \mathcal{L}_{\text{traj}} + \lambda_{\text{head}} \mathcal{L}_{\text{head}} + \lambda_U \mathcal{L}_U + \alpha \mathcal{L}_{\text{aux}}. \quad (5)$$

\mathcal{L}_{aux} denotes the sum of lightweight auxiliary classification losses used only during training to regularize the shared en-

coders. We use $\lambda_{\text{traj}} = \lambda_{\text{head}} = \lambda_U = 1$, $\lambda_{\text{var}} = 0.3$, and $\alpha = 0.3$.

3.3. Implementation Details

We train on a single NVIDIA RTX 4090 with AdamW [31], using a 2-epoch linear warm-up followed by cosine annealing over 200 epochs. The maximum learning rate is 5×10^{-5} with weight decay 1×10^{-4} and batch size 16. To keep the training time under control, we precompute and cache DINoV2 features at the module level where subsequent training uses these cached features and the backbone remains frozen.

4. Cognition-aware Egocentric Navigation (CEN) Dataset

As discussed in Section 2, there is currently no publicly available dataset to support research into egocentric human navigation with cognitive factors. We therefore introduce CEN, a multimodal egocentric navigation dataset combining rich sensory inputs with moment-to-moment annotations of perceived path uncertainty. We detail the data-collection pipeline and dataset statistics below.

4.1. Data Collection

Hardware. To accommodate the distinct characteristics of indoor and outdoor environments, we employ two complementary setups. For outdoors, we use Tobii Pro Glasses capturing 20fps RGB with high-quality binocular gaze and 6-axis IMU commonly used across studies [41], and a reliable Garmin handheld GPS providing precise global positions. For indoor scenarios, we use Project Aria glasses [13] that capture 20fps RGB video with accurate SLAM via two monochrome cameras, eye-tracking, and an IMU sensor. In both settings, participants hold an Xbox controller ¹ to continuously self-report perceived path uncertainty on a normalized [0,1] scale.

Recording procedure. Before each session, participants were briefed on the study goals and received a tutorial on how to continuously report perceived uncertainty with the joystick for full range. Participants were explicitly instructed to perform route-finding behaviors when uncertain such as scanning the surroundings for cues, confirming signage or landmarks, and were reminded to check for passing vehicles before crossing streets. During recording, participants navigated from a fixed starting point through an identical sequence of waypoints per scenario toward predefined goals for each scenario. A researcher trailed each participant to present the next waypoint image upon arrival at previous one to ensure proper task progression.

Data processing. Outdoor recordings from Tobii Pro Glasses are processed in Tobii Pro Lab² and exported as .tsv files with multimodal streams including 2D gaze coordinates, 6-axis IMU signals, and egocentric videos. Trajectories are obtained from GPS logs in .gpx files and are smoothed with a Savitzky–Golay filter [51]. Joystick signals are saved as .csv with magnitude of each press. Indoor sessions are stored in .vrs files and processed with Aria Machine Perception Services³ to extract RGB video, 6D head-pose trajectories, scene point clouds, and eye-gaze estimates. All recordings are synchronized to a 10 Hz timeline via down-sampling with nearest neighbor or interpolation. We additionally annotate videos with behavior types and environment categories to provide labels for supervised learning and validation.

Privacy. All recordings were de-identified by blurring faces and removing audio to protect privacy of participants.

4.2. Dataset Statistics.

The dataset comprises approximately 6 hours from 17 participants with total 226k RGB frames across 42 distinct sites. Diverse sites were selected across indoor and outdoor

settings, including university campuses, healthcare facilities, urban commercial streets, and natural routes. The sites are recorded at varied times of day with vary lighting, crowding, and traffic. Wayfinding routes are designed to integrate four uncertainty-inducing spatial types. We further annotate three label groups for stratified analysis and auxiliary supervision. Labels were selected from pilot observations and theory that cause choice difficulty and subsequent behavioral responses. Environment types include multiple-route junctions (JCT), occluded/poor-signage segments (OCC), multi-level/vertical transitions (MULT), dynamic/crowded areas (CROWD), and spatial transitions/sudden changes (ST); trajectory behaviors include hesitation/pausing (HES), wrong turn (WRONG), and backtrack (BACK); head-movement behaviors include information gathering (SCAN), information confirmation/cross-check (CONFIRM), and look-back (LB).

5. Experiments

We evaluate EgoCogNav with baselines in Section 5.1.1 and ablate key design choices in Section 5.1.2. We also provide qualitative analyses that visualize trajectory and head-pose forecasts and uncertainty signals in Section 5.2. Finally, we discuss limitations and future directions in Section 5.3. All results are reported on a held-out test set with environments unseen during training.

5.1. Quantitative Evaluation

Metrics. For trajectory, we report Average Displacement Error (ADE), which captures the mean distance between predicted and actual positions at each timestep; and Final Displacement Error (FDE), which measures the distance at the trajectory endpoint. we evaluate the L1 loss [43] used during training for head rotations. As for uncertainty, we report mean absolute error (MAE), Spearman rank correlation coefficient [18]. The High-U precision reports how often the model’s top-20% uncertainty moments coincide with labeled difficulty events, and and assess how it links to labeled behaviors. ΔU measures the average elevation of uncertainty during behavior onsets relative to neutral periods, while the reported effect size quantifies the magnitude of this elevation. We also assess mean uncertainty across behavioral contexts and report the standardized effect size characterizing its association with labeled motion and head-movement events.

5.1.1. Comparison with Baselines

Baselines. Since this is a novel task, there is limited baselines to the best of our knowledge. The closest related works [43, 46, 59] are either pre-print or have no public released code. As a result, we compare against three baselines: (1) Constant Velocity (Const_Vel) [38], which extrapolates future body-frame translation from the last linear

¹<https://xboxdesignlab.xbox.com/en-us/controllers/xbox-wireless-controller>

²<https://www.tobii.com/products/software/behavior-research-software/tobii-pro-lab>

³<https://huggingface.co/projectaria>

| Method | All Scenarios | | | High Uncertainty Scenarios | | |
|---------------|---------------|-------------|--------------|----------------------------|-------------|--------------|
| | ADE ↓ | FDE ↓ | L1 (head) ↓ | ADE ↓ | FDE ↓ | L1 (head) ↓ |
| Const_Vel | 0.19 | 0.33 | 0.098 | 0.18 | 0.34 | 0.101 |
| Lin_Ext | — | — | 0.174 | — | — | 0.195 |
| M_Transformer | 0.16 | 0.29 | 0.091 | 0.18 | 0.29 | 0.094 |
| EgoCast [14] | 0.14 | 0.25 | 0.086 | 0.15 | 0.22 | 0.088 |
| Ours | 0.12 | 0.22 | 0.082 | 0.13 | 0.21 | 0.083 |

Table 1. **Baseline comparison.** Trajectory (ADE/FDE) and head rotation (L1) on the full test set and on a top 20% highest uncertainty subset.

velocity and future head rotation from the last angular velocity, (2) Linear Extrapolation (Lin_Ext) [43], which fits a per-axis linear model to the past translation and rotation sequences and projects them into the future, (3) a standard Multimodal Transformer (M_Transformer) baseline that uses the same inputs and training protocol as our model but performs early fusion by concatenating stream embeddings with a single temporal transformer decoder, followed by two linear heads that predict trajectory and head motion in parallel, and (4) EgoCast [14] where we adapt its forecasting module which was originally designed for full-body pose to our trajectory and head-motion prediction settings with more layers.

As for perceived uncertainty prediction, we compare with two baselines: (1) an EMU-entropy (EMU) theory proxy, which computes two signals of perceptual ambiguity from visual scenes and behavioral variability from short-horizon motion, and learns a linear combination to the human uncertainty label; and (2) a PATH-U-adapted (PATH_U) [61] model, as it was originally designed for indoor wayfinding using signage, we adapt it to the egocentric setting by composing a 5-dimensional feature vectors capturing decision complexity and behavioral variability (e.g., junction count, occlusion/poor-signage count, goal distance), and fitting a linear regressor to predict perceived uncertainty.

Results. The comparison results are presented in Table 1. On the high-uncertainty subset, our model achieves the strongest performance for both trajectory and head-orientation forecasting, while on the full set, it remains competitive on head rotation and leads on trajectory prediction metrics. Table 2 shows that our uncertainty estimates are more accurate than theory- or rule-based baselines and can concentrate earlier around behavior onsets, and it also produces higher precision for top-uncertainty moments with larger effect sizes. The breakdown in Table 3 confirms that uncertainty rises most for navigation difficulties (e.g., wrong turns, backtracks) and is moderately elevated for information-seeking (hesitation, scanning) which shows cognitive expectations for uncertainty-eliciting sce-

narios.

5.1.2. Ablation Study

We conduct ablations on key architectural choices and input modalities and summarize results in Table 4. As contribution of our framework, we assess the impact of the trajectory loss and the auxiliary environment/behavior classification losses. We can see both have consistent improvements over the vanilla architecture on the validation set. The horizon-weighted trajectory loss especially reduces late-step errors to improve anticipatory performance, while the auxiliary heads modestly enhances head-rotation error and reduces variance which indicates effective regularization. Additionally, given the model’s modular design, we also compare modality inputs and observe gains when using the full multimodal input sequences.

5.2. Qualitative Evaluation

We visualize predictions alongside ground truth for trajectories and head motion, and overlay uncertainty as a color-coded intensity along the predicted path shown in Fig. 3. Overall, our model closely tracks ground-truth trajectories and head orientations across conditions while producing uncertainty values that align with decision difficulty environments. In multi-junction scenes, we observe elevated uncertainty before hesitation and scanning. And in occlusion-heavy cases, uncertainty peaks before backtracking. Conversely, in well-specified corridors with clear sight-lines, uncertainty remains low and motion is smooth. These patterns qualitatively support our analysis and indicate that the model captures both route-finding behaviors, and their coupling with perceived uncertainty. From an environment-centric perspective, we observe that scenes rated by participants as more confusing or cognitively demanding can systematically induce higher predicted uncertainty, while visually simple regions correspond to low predicted uncertainty. This alignment between environmental structures and subjective feelings from model outputs suggests that EgoCog-Nav captures not only route-finding behaviors but also how different environments are experienced.

| Method | Uncertainty Accuracy | | Behavioral Correlation | | |
|-------------|----------------------|-----------------|---------------------------------|---------------------|------------------------|
| | MAE \downarrow | $\rho \uparrow$ | Precision for high U \uparrow | $\Delta U \uparrow$ | Effect Size \uparrow |
| EMU | 0.38 | 0.17 | 0.20 | 0.05 | 0.75 |
| PATH_U [61] | 0.37 | 0.13 | 0.18 | 0.04 | 0.70 |
| Ours | 0.23 | 0.64 | 0.45 | 0.10 | 0.85 |

Table 2. **Uncertainty prediction.** We evaluate MAE and Spearman ρ for uncertainty prediction accuracy. The precision measures those among the highest 20% uncertainty moments, and ΔU is the mean uncertainty elevation during behaviors compared to neutral behavioral settings. The effect size is large among uncertainty elevation and onset of behaviors.

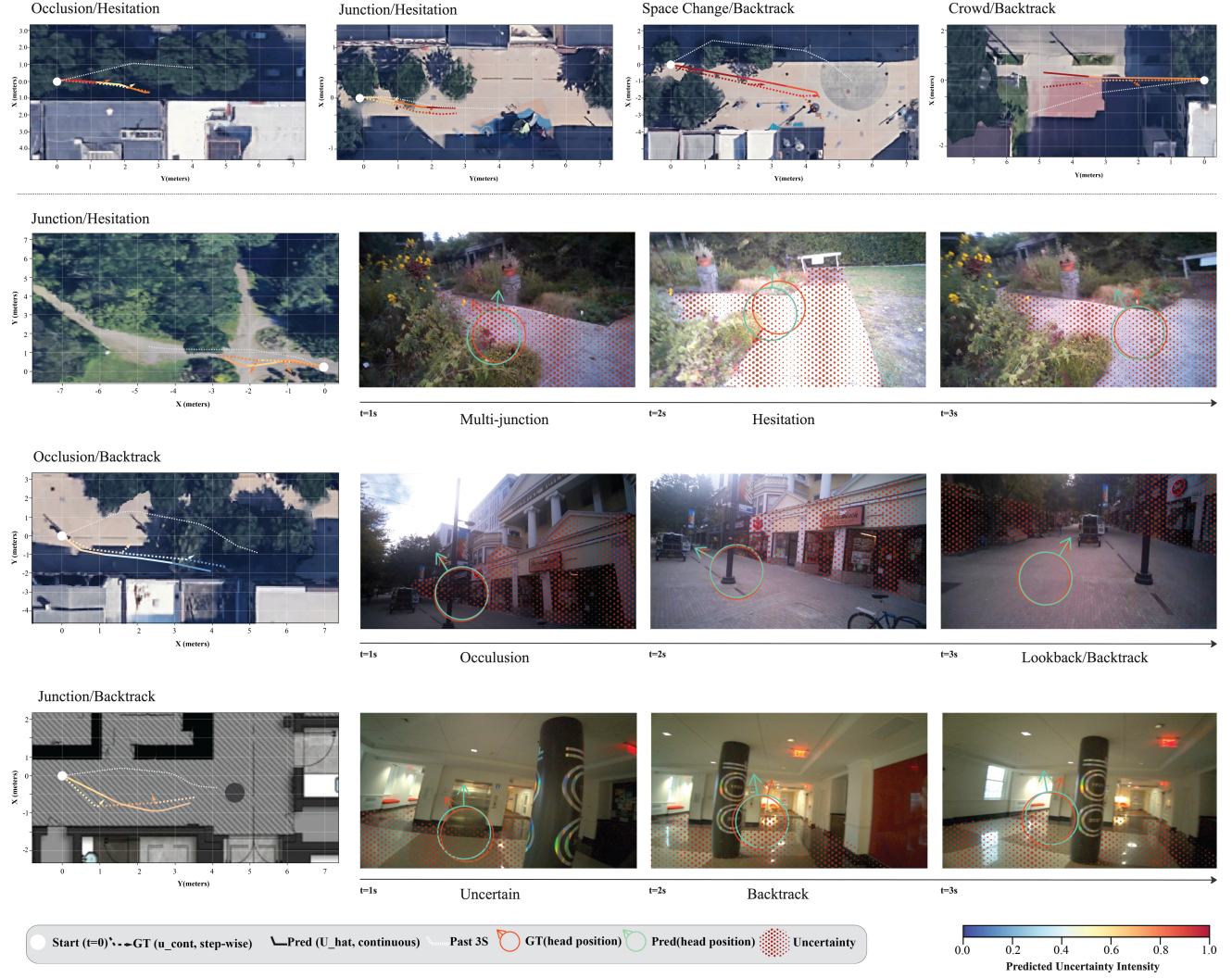


Figure 3. **Qualitative visualizations.** The top row presents BEV examples under high-uncertainty and behavior-eliciting scenarios. For each scenario on the bottom row, the left panel shows a BEV overlay with past trajectory (gray), ground-truth future, predicted future, and overlaid path uncertainty. The right panels show time-aligned egocentric frames ($t+1$ to $t+3s$) with ground-truth (red) and predicted (green) head positions. Environments were also highlighted with red dots for those that trigger uncertain behaviors.

Failure cases. We also identify failure cases as illustrated in Fig. 4. In the first scenario, the participant suspected a wrong turn due to heavy occlusion and backtracked to

seek an alternative route. Our model instead predicted a return along the same path segment rather than backtracking to other decision points. This indicates insufficient use

| Behavior Type | Mean Uncertainty | Effect Size \uparrow |
|----------------------|------------------|------------------------|
| HES (Hesitation) | 0.39 | 0.52 |
| WRONG (Wrong Turn) | 0.62 | 1.58 |
| BACK (Backtrack) | 0.56 | 1.21 |
| SCAN (Head Scanning) | 0.39 | 0.68 |
| LB (Look-back) | 0.58 | 1.35 |
| Any | 0.41 | 0.85 |
| Neutral | 0.31 | — |

Table 3. **Uncertainty-behavioral analysis.** Mean predicted uncertainty and effect size for behavioral event type.

| Variant | ADE \downarrow | FDE \downarrow | L1 (head) \downarrow |
|---------------------------|------------------|------------------|------------------------|
| Full (Ours) | 0.12 | 0.22 | 0.082 |
| without auxiliary losses | 0.14 | 0.24 | 0.086 |
| without trajectory losses | 0.16 | 0.28 | 0.087 |
| video+motion | 0.14 | 0.23 | 0.085 |
| video-only | 0.15 | 0.25 | 0.088 |
| motion-only | 0.17 | 0.28 | 0.093 |

Table 4. **Ablation study.** Each design choice helps improve the performance.

of long-horizon visual context and episodic scene memory. In the second example, although the predicted path heads in the correct direction, it fails to capture the brief hesitation and look-back behaviors triggered by the changing scene context. These failure cases emphasize the need for stronger global context beyond the immediate scene representations and for explicit multi-hypothesis futures when comparable uncertainty covers multiple plausible routes.

5.3. Limitations and Future Work

There are several limitations noted. First, when salient cues are outside the camera frustum or are heavily occluded, the model operates with partial scene knowledge and degrades performance. Future work can incorporate richer 3D/semantic context to improve disambiguation at complex environments. Second, we predict a single best trajectory and head sequence, and can utilize generative models to sample a distribution of futures to better capture diverse navigation styles under similar cognitive states. Last, this work features uncertainty as main cognitive factor and future work will incorporate additional cognitive/experiential signals such as affect and spatial memory and extend from short-horizon forecasting to hierarchical, longer-horizon planning.

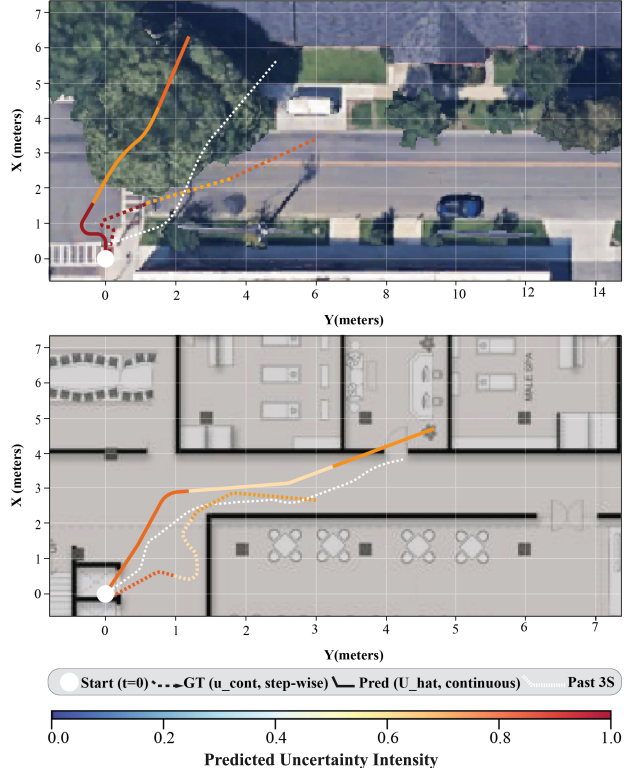


Figure 4. **Failure cases.** Two failure cases highlight limits in long-horizon scene memory and the lack of multi-hypothesis futures.

6. Conclusion

In this paper we present several key contributions to the goal of cognition-aware egocentric navigation. First, we introduce the challenging task of jointly forecasting body-centered trajectory, head motion, and perceived path uncertainty from the basis of multimodal input. This formulation enables the model to reason not only about future motion but also about underlying cognitive states to explain onset behaviors and environmental evaluation. Second, we propose EgoCogNav, an architecture that effectively integrates scene features and sensory cues to accurately forecast human motion. To support this task, we collect the CEN dataset, a 6-hour collection of real-world recordings across 42 diverse environments with synchronized video, IMU, gaze, and self-reported uncertainty. Our results indicate that EgoCogNav learns the coupling between perception, perceived uncertainty, and human-like navigation behaviors while generalizing to unseen environments during training. We also discussed the limitations of the project and important future work that is needed toward real-world deployment in social and assistive navigation technologies.

References

[1] Hiroyasu Akada, Jian Wang, Vladislav Golyanik, and Christian Theobalt. 3d human pose perception from egocentric stereo videos. In *Proceedings of the IEEE/CVF Conference on computer vision and pattern recognition*, pages 767–776, 2024. 2

[2] Alexandre Alahi, Kratarth Goel, Vignesh Ramanathan, Alexandre Robicquet, Li Fei-Fei, and Silvio Savarese. Social lstm: Human trajectory prediction in crowded spaces. In *Proceedings of the IEEE conference on computer vision and pattern recognition*, pages 961–971, 2016. 2

[3] Ron Amit, Ron Meir, and Kamil Ciosek. Discount factor as a regularizer in reinforcement learning. In *International conference on machine learning*, pages 269–278. PMLR, 2020. 4

[4] Inhwan Bae, Young-Jae Park, and Hae-Gon Jeon. Singulartrajectory: Universal trajectory predictor using diffusion model. In *Proceedings of the IEEE/CVF Conference on Computer Vision and Pattern Recognition*, pages 17890–17901, 2024. 2

[5] Prithviraj Banerjee, Sindi Shkodrani, Pierre Moulon, Shreyas Hampali, Shangchen Han, Fan Zhang, Linguang Zhang, Jade Fountain, Edward Miller, Selen Basol, et al. Hot3d: Hand and object tracking in 3d from egocentric multi-view videos. In *Proceedings of the Computer Vision and Pattern Recognition Conference*, pages 7061–7071, 2025. 3

[6] Tibor Bosse, Mark Hoogendoorn, Michel CA Klein, Jan Treur, C Natalie Van Der Wal, and Arlette Van Wissen. Modelling collective decision making in groups and crowds: Integrating social contagion and interacting emotions, beliefs and intentions. *Autonomous Agents and Multi-Agent Systems*, 27(1):52–84, 2013. 1

[7] Mathilde Caron, Hugo Touvron, Ishan Misra, Hervé Jégou, Julien Mairal, Piotr Bojanowski, and Armand Joulin. Emerging properties in self-supervised vision transformers. In *Proceedings of the IEEE/CVF international conference on computer vision*, pages 9650–9660, 2021. 1, 3

[8] Dima Damen, Hazel Doughty, Giovanni Maria Farinella, Sanja Fidler, Antonino Furnari, Evangelos Kazakos, Davide Moltisanti, Jonathan Munro, Toby Perrett, Will Price, et al. Scaling egocentric vision: The epic-kitchens dataset. In *Proceedings of the European conference on computer vision (ECCV)*, pages 720–736, 2018. 3

[9] Melissa De Iuliis, Edoardo Battegazzorre, Marco Donameschi, Gian Paolo Cimellaro, and Andrea Giuseppe Bottino. Large scale simulation of pedestrian seismic evacuation including panic behavior. *Sustainable Cities and Society*, 94: 104527, 2023. 1

[10] Ann Sloan Devlin. Wayfinding in healthcare facilities: Contributions from environmental psychology. *Behavioral sciences*, 4(4):423–436, 2014. 1, 2

[11] Rohit K Dubey, Samuel S Sohn, Christoph Hoelscher, and Mubbashir Kapadia. Fusion-based wayfinding prediction model for multiple information sources. In *2019 22th international conference on information fusion (FUSION)*, pages 1–8. IEEE, 2019. 1

[12] Lydie Edward, Domitile Lourdeaux, and Jean-Paul Barthes. Cognitive modeling of virtual autonomous intelligent agents integrating human factors. In *2009 IEEE/WIC/ACM International Joint Conference on Web Intelligence and Intelligent Agent Technology*, pages 353–356. IEEE, 2009. 1

[13] Jakob Engel, Kiran Somasundaram, Michael Goesele, Albert Sun, Alexander Gamino, Andrew Turner, Arjang Talatoff, Arnie Yuan, Bilal Souti, Brighid Meredith, et al. Project aria: A new tool for egocentric multi-modal ai research. *arXiv preprint arXiv:2308.13561*, 2023. 3, 5

[14] Maria Escobar, Juanita Puentes, Cristhian Forigua, Jordi Pont-Tuset, Kevis-Kokitsi Maninis, and Pablo Arbelaez. Egocast: Forecasting egocentric human pose in the wild. In *2025 IEEE/CVF Winter Conference on Applications of Computer Vision (WACV)*, pages 5831–5841. IEEE, 2025. 6

[15] Anna Charisse Farr, Tristan Kleinschmidt, Prasad Yarlagadda, and Kerrie Mengersen. Wayfinding: A simple concept, a complex process. *Transport Reviews*, 32(6):715–743, 2012. 1

[16] Kristen Grauman, Andrew Westbury, Eugene Byrne, Zachary Chavis, Antonino Furnari, Rohit Girdhar, Jackson Hamburger, Hao Jiang, Miao Liu, Xingyu Liu, et al. Ego4d: Around the world in 3,000 hours of egocentric video. In *Proceedings of the IEEE/CVF conference on computer vision and pattern recognition*, pages 18995–19012, 2022. 3

[17] Tianpei Gu, Guangyi Chen, Junlong Li, Chunze Lin, Yongming Rao, Jie Zhou, and Jiwen Lu. Stochastic trajectory prediction via motion indeterminacy diffusion. In *Proceedings of the IEEE/CVF conference on computer vision and pattern recognition*, pages 17113–17122, 2022. 1, 2

[18] Jan Hauke and Tomasz Kossowski. Comparison of values of pearson’s and spearman’s correlation coefficients on the same sets of data. *Quaestiones geographicae*, 30(2):87–93, 2011. 5

[19] Noriaki Hirose, Dhruv Shah, Ajay Sridhar, and Sergey Levine. Sacson: Scalable autonomous control for social navigation. *IEEE Robotics and Automation Letters*, 9(1):49–56, 2023. 1

[20] Jacob B Hirsh, Raymond A Mar, and Jordan B Peterson. Psychological entropy: a framework for understanding uncertainty-related anxiety. *Psychological review*, 119(2): 304, 2012. 1, 2, 3

[21] Rong Huang, Xuan Zhao, Yufei Yuan, Qiang Yu, Chengqing Liu, and Winnie Daamen. Modeling pedestrian tactical and operational decisions under risk and uncertainty: A two-layer model framework. *IEEE Transactions on Intelligent Transportation Systems*, 24(5):5259–5281, 2023. 2

[22] Ajay Jain, Sergio Casas, Renjie Liao, Yuwen Xiong, Song Feng, Sean Segal, and Raquel Urtasun. Discrete residual flow for probabilistic pedestrian behavior prediction. In *Conference on Robot Learning*, pages 407–419. PMLR, 2020. 1

[23] Jaewoo Jeong, Seohee Lee, Daehee Park, Giwon Lee, and Kuk-Jin Yoon. Multi-modal knowledge distillation-based human trajectory forecasting. In *Proceedings of the Computer Vision and Pattern Recognition Conference*, pages 24222–24233, 2025. 1

[24] S Didem Kaya, Y Yalcin Ileri, and Aydan Yuceler. Importance of hospital way-finding system on patient satisfac-

tion. In *Business Challenges in the Changing Economic Landscape-Vol. 2: Proceedings of the 14th Eurasia Business and Economics Society Conference*, pages 33–40. Springer, 2016. 1

[25] Parth Kothari, Sven Kreiss, and Alexandre Alahi. Human trajectory forecasting in crowds: A deep learning perspective. *IEEE Transactions on Intelligent Transportation Systems*, 23(7):7386–7400, 2021. 2

[26] Henrik Kretzschmar, Markus Spies, Christoph Sprunk, and Wolfram Burgard. Socially compliant mobile robot navigation via inverse reinforcement learning. *The International Journal of Robotics Research*, 35(11):1289–1307, 2016. 1

[27] Jiaman Li, Karen Liu, and Jiajun Wu. Ego-body pose estimation via ego-head pose estimation. In *Proceedings of the IEEE/CVF Conference on Computer Vision and Pattern Recognition*, pages 17142–17151, 2023. 2

[28] Yin Li, Miao Liu, and James M Rehg. In the eye of the beholder: Gaze and actions in first person video. *IEEE transactions on pattern analysis and machine intelligence*, 45(6):6731–6747, 2021. 3

[29] Yanghao Li, Tushar Nagarajan, Bo Xiong, and Kristen Grauman. Ego-exo: Transferring visual representations from third-person to first-person videos. In *Proceedings of the IEEE/CVF Conference on Computer Vision and Pattern Recognition*, pages 6943–6953, 2021. 3

[30] Yuan-Ming Li, Wei-Jin Huang, An-Lan Wang, Ling-An Zeng, Jing-Ke Meng, and Wei-Shi Zheng. Egoexo-fitness: Towards egocentric and exocentric full-body action understanding. In *European Conference on Computer Vision*, pages 363–382. Springer, 2024. 3

[31] Ilya Loshchilov and Frank Hutter. Decoupled weight decay regularization. *arXiv preprint arXiv:1711.05101*, 2017. 4

[32] Zhaoyang Lv, Nicholas Charron, Pierre Moulon, Alexander Gumno, Cheng Peng, Chris Sweeney, Edward Miller, Huixuan Tang, Jeff Meissner, Jing Dong, et al. Aria everyday activities dataset. *arXiv preprint arXiv:2402.13349*, 2024. 3

[33] Lingni Ma, Yuting Ye, Fangzhou Hong, Vladimir Guzov, Yifeng Jiang, Rowan Postyeni, Luis Pesqueira, Alexander Gumno, Vijay Baiyya, Hyo Jin Kim, et al. Nymeria: A massive collection of multimodal egocentric daily motion in the wild. In *European Conference on Computer Vision*, pages 445–465. Springer, 2024. 3

[34] Roger L Mackett. Mental health and wayfinding. *Transportation research part F: traffic psychology and behaviour*, 81:342–354, 2021. 1

[35] Takahiro Maeda and Norimichi Ukita. Fast inference and update of probabilistic density estimation on trajectory prediction. In *Proceedings of the IEEE/CVF international conference on computer vision*, pages 9795–9805, 2023. 2

[36] Weibo Mao, Chenxin Xu, Qi Zhu, Siheng Chen, and Yanfeng Wang. Leapfrog diffusion model for stochastic trajectory prediction. In *Proceedings of the IEEE/CVF conference on computer vision and pattern recognition*, pages 5517–5526, 2023. 1, 2

[37] Tsubasa Maruyama, Satoshi Kanai, Hiroaki Date, and Mitsuori Tada. Simulation-based evaluation of ease of wayfinding using digital human and as-is environment models. *PRS International Journal of Geo-Information*, 6(9):267, 2017. 1

[38] Christoforos Mavrogiannis, Patrícia Alves-Oliveira, Wil Thomason, and Ross A Knepper. Social momentum: Design and evaluation of a framework for socially competent robot navigation. *ACM Transactions on Human-Robot Interaction (THRI)*, 11(2):1–37, 2022. 1, 5

[39] Christoforos Mavrogiannis, Francesca Baldini, Allan Wang, Dapeng Zhao, Pete Trautman, Aaron Steinfeld, and Jean Oh. Core challenges of social robot navigation: A survey. *ACM Transactions on Human-Robot Interaction*, 12(3):1–39, 2023. 2

[40] Duc M Nguyen, Mohammad Nazeri, Amirreza Payandeh, Aniket Datar, and Xuesu Xiao. Toward human-like social robot navigation: A large-scale, multi-modal, social human navigation dataset. In *2023 IEEE/RSJ International Conference on Intelligent Robots and Systems (IROS)*, pages 7442–7447. IEEE, 2023.

[41] V Onkhar, D Dodou, and JCF De Winter. Evaluating the tobii pro glasses 2 and 3 in static and dynamic conditions. *Behavior Research Methods*, 56(5):4221–4238, 2024. 5

[42] Maxime Oquab, Timothée Darcet, Théo Moutakanni, Huy Vo, Marc Szafraniec, Vasil Khalidov, Pierre Fernandez, Daniel Haziza, Francisco Massa, Alaeldin El-Nouby, et al. Dinov2: Learning robust visual features without supervision. *arXiv preprint arXiv:2304.07193*, 2023. 1, 3

[43] Boxiao Pan, Adam W Harley, Francis Engelmann, C Karen Liu, and Leonidas J Guibas. Lookout: Real-world humanoid egocentric navigation. In *Proceedings of the IEEE/CVF International Conference on Computer Vision*, pages 24977–24988, 2025. 2, 3, 4, 5, 6

[44] Xiaoshan Pan. *Computational modeling of human and social behaviors for emergency egress analysis*. Stanford University, 2006. 1

[45] Amir Ehsan Pouyan, Abdul Hamid Ghanbaran, Abbas Hosseini-zadeh, and Amir Shakibamanesh. The elderly wayfinding performance in an informative healthcare design indoors. *Journal of Building Engineering*, 87:108843, 2024. 1, 2

[46] Jianing Qiu, Lipeng Chen, Xiao Gu, Frank P-W Lo, Ya-Yen Tsai, Jiankai Sun, Jiaqi Liu, and Benny Lo. Egocentric human trajectory forecasting with a wearable camera and multi-modal fusion. *IEEE Robotics and Automation Letters*, 7(4):8799–8806, 2022. 5

[47] Martin Raubal. Human wayfinding in unfamiliar buildings: a simulation with a cognizing agent. *Cognitive Processing*, 2(3):363–388, 2001. 1, 2

[48] Martin Raubal and Michael Worboys. A formal model of the process of wayfinding in built environments. In *International conference on spatial information theory*, pages 381–399. Springer, 1999. 1

[49] Saeed Saadatnejad, Yang Gao, Kaouthar Messaoud, and Alexandre Alahi. Social-transmotion: Promptable human trajectory prediction. *arXiv preprint arXiv:2312.16168*, 2023. 2

[50] Tim Salzmann, Hao-Tien Lewis Chiang, Markus Ryll, Dorsa Sadigh, Carolina Parada, and Alex Bewley. Robots that can see: Leveraging human pose for trajectory prediction. *IEEE Robotics and Automation Letters*, 8(11):7090–7097, 2023. 1

[51] Ronald W Schafer. What is a savitzky-golay filter?[lecture notes]. *IEEE Signal processing magazine*, 28(4):111–117, 2011. 5

[52] Christoph Schöller and Alois Knoll. Flomo: Tractable motion prediction with normalizing flows. In *2021 IEEE/RSJ International Conference on Intelligent Robots and Systems (IROS)*, pages 7977–7984. IEEE, 2021. 2

[53] Daeun Song, Jing Liang, Amirreza Payandeh, Amir Hossain Raj, Xuesu Xiao, and Dinesh Manocha. Vlm-social-nav: Socially aware robot navigation through scoring using vision-language models. *IEEE Robotics and Automation Letters*, 2024. 1

[54] Hao Tang, Kevin J Liang, Kristen Grauman, Matt Feiszli, and Weiyao Wang. Egotracks: A long-term egocentric visual object tracking dataset. *Advances in Neural Information Processing Systems*, 36:75716–75739, 2023. 3

[55] Denis Tome, Patrick Peluse, Lourdes Agapito, and Hernan Badino. xr-egopose: Egocentric 3d human pose from an hmd camera. In *Proceedings of the IEEE/CVF International Conference on Computer Vision*, pages 7728–7738, 2019. 2

[56] Koen Vellenga, H Joe Steinhauer, Göran Falkman, and Tomas Björklund. Evaluation of video masked autoencoders’ performance and uncertainty estimations for driver action and intention recognition. In *Proceedings of the IEEE/CVF Winter Conference on Applications of Computer Vision*, pages 7429–7437, 2024. 1

[57] Nick Walker, Christoforos Mavrogiannis, Siddhartha Srinivasan, and Maya Cakmak. Influencing behavioral attributions to robot motion during task execution. In *Conference on Robot Learning*, pages 169–179. PMLR, 2022. 1

[58] Jian Wang, Diogo Luvizon, Weipeng Xu, Lingjie Liu, Kripasindhu Sarkar, and Christian Theobalt. Scene-aware egocentric 3d human pose estimation. In *Proceedings of the IEEE/CVF Conference on Computer Vision and Pattern Recognition*, pages 13031–13040, 2023. 3

[59] Weizhuo Wang, C Karen Liu, and Monroe Kennedy III. Egnav: Egocentric scene-aware human trajectory prediction. *arXiv preprint arXiv:2403.19026*, 2024. 2, 3, 5

[60] Wei Xie, Eric Wai Ming Lee, and Yiu Yin Lee. Simulation of spontaneous leader-follower behaviour in crowd evacuation. *Automation in Construction*, 134:104100, 2022. 2

[61] Qi Yang, Rohit K Dubey, and Saleh Kalantari. Path-u: A data-driven agent-based wayfinding model incorporating perceived path uncertainty and cognitive strategies in unfamiliar indoor environments. In *Building Simulation*, pages 449–471. Springer, 2025. 1, 3, 6, 7

[62] Brent Yi, Vickie Ye, Maya Zheng, Yunqi Li, Lea Müller, Georgios Pavlakos, Yi Ma, Jitendra Malik, and Angjoo Kanazawa. Estimating body and hand motion in an ego-sensed world. In *Proceedings of the Computer Vision and Pattern Recognition Conference*, pages 7072–7084, 2025. 2

[63] Yi Zhou, Connelly Barnes, Jingwan Lu, Jimei Yang, and Hao Li. On the continuity of rotation representations in neural networks. In *Proceedings of the IEEE/CVF conference on computer vision and pattern recognition*, pages 5745–5753, 2019. 3

[64] Runhe Zhu, Burcin Becerik-Gerber, Jing Lin, and Nan Li. Behavioral, data-driven, agent-based evacuation simulation for building safety design using machine learning and discrete choice models. *Advanced Engineering Informatics*, 55:101827, 2023. 2

[65] Yu Zhu, Tao Chen, Ning Ding, Mohcine Chraibi, and Wei-Cheng Fan. Follow people or signs? a novel way-finding method based on experiments and simulation. *Physica A: Statistical Mechanics and its Applications*, 573:125926, 2021. 1